Indian Journal of Engineering & Materials Sciences
Vol. 29, August 2022, pp. 445-458
DOI: 10.56042/ijems.v29i4.47313

Performance evaluation and multi-response hybrid optimization of grinding assisted rotary disk ECDM during cutting of Al-6063 SiCp MMC

Navin Kumar Jha[a], Sandeep Kumar[b]*, Rajendra Kumar Arya[c], Akshay Dvivedi[d], & Shivanna Rajesha[a]

[a]Department of Mechanical Engineering, JSS Academy of Technical Education, Noida 201 301, India

[b]Industrial & Production Engineering Department, College of Technology, G.B. Pant University of Agriculture & Technology, Pantnagar 263 145, India

[c]Mechanical Engineering Department, Indian Institute of Technology Bombay 400 076, India

[d]Mechanical and Industrial Engineering Department, Indian Institute of Technology, Roorkee, Uttrakhand 247 667, India

Received: 10 March 2021; Accepted: 21 September 2021

The Metal Matrix Composites (MMCs) are being used in many applications, including aerospace, shipbuilding, and defence industries owing to their high strength to weight ratio. However, the machining of these materials is still challenging, necessitating advanced machining techniques. The current investigation aimed to analyze the performance of the grinding-assisted rotary disc-electrochemical discharge machining (GA-RD-ECDM) process during cutting Al-6063 SiCp MMC. Detailed experimentation was performed to study the energy interaction behavior and effect of input process variables viz. applied voltage, pulse on time, electrolyte concentration, and disc rotation speed on performance measures. The responses selected were taper, overcut (WOC), and Materials Removal Rate (MRR). The experimentation work was performed by adopting response surface methodology. Regression models were developed and statistically analyzed through analysis of variance (ANOVA). Eventually, the GA-RD-ECDM process was optimized using the VIKOR methodology of multi-criteria decision-making by considering accuracy and productivity simultaneously to obtain minimum taper and WOC and maximum MRR. The results of ANOVA revealed that input variables were statistically significant. Applied voltage most significantly affects the performance of the GA-RD-ECDM process performance. The optimal values of input process variables obtained by VIKOR method were applied voltage = 100 V, pulse-on time = 3 ms, Electrolyte concentration = 18% wt/vol. and disc rotation speed = 30 rpm. The present work can provide a productive solution for cutting of difficult-to-cut materials. Thus, in future, the GA-RD-ECDM process can be investigated for other advanced materials (i.e., glass, polymer composites and ceramics) for fabrication of microchannels for microfluidic applications.

Keywords: GA-RD-ECDM, Materials Matrix Composites (MMCs), Materials Removal Rate (MRR), Taper, Overcut, VIKOR, MCDM

1 Introduction

Metal matrix composites (MMCs) have been using in many industrial applications, including microelectronics, aerospace, optical and tribology etc.[1]The superior properties of MMCs viz, lightweight, high strength, resistance to corrosion, and high specific stiffness make them suitable candidate material for aforesaid applications.[2]MMCs are the mixture of two or more constituents (macro/micro) having a distinct interface.[3] The constituents are known as matrix and reinforcement. The metal matrix (i.e., aluminium, copper, magnesium etc.) is reinforced by hard particles such as SiC, Al_2O_3, B_4C etc. The properties of MMCs can be altered as per the requirements/application by modifying the proportions of the constituents. Al/SiC is the most popular and versatile MMC among all. This combination is preferred due to the high thermal conductivity, lesser aluminum matrix density, and high hardness of SiC reinforcement.[4] The industrial application of Al/SiC MMC includes heat sinks fabricated on printed circuit boards and electronic packaging. Further, within Al alloys, Al-6063 is always preferred by the users owing its higher thermal conductivity, which is extensively used to make electrical components and heat sinks, etc. However, the superior properties of MMCs make them difficult to cut, specifically in high accuracy machining. Several investigations have been performed to develop a cost-effective method for the generation of dimensionally accurate intricate shapes on MMCs. Nevertheless, the desires shape with the desired accuracy is still cannot be achieved without using the secondary processing of MMCs. In order to fulfil this requirement, both traditional and advanced machining methods are being used.[5] Since the reinforcement (i.e., SiC) has very high hardness, that causes severe tool wear

*Corresponding author(E-mail: sandeepkumar71@gmail.com)

during machining of MMCs by conventional machining methods.[6] High tool wear increases the additional cost of the tool and deteriorates the accuracy of the machined component. Due to this reason, conventional machining is less preferred for machining of MMCs. Though the advanced machining methods are popular for the needed application, they also have different limitations, such as high cost, thermal damage, high power consumption, and sometimes low material removal rate. Considering all the advanced machining methods, electrochemical discharge machining (ECDM) is a hybrid version of two popular machining processes (i.e., electro-chemical machining (ECM) and electro-discharge machining (EDM)).[7] The ECDM exhibits a higher machining rate as compare to EDM and ECM separately.[8]Moreover, it exhibits better form accuracy of features as compare to AWJM. In this process, an electrolyte bath is used, in which two electrodes (i.e.,tool and auxiliary) are dipped. The tool electrode is made the cathode, and the auxiliary electrode is made the anode. The connection is established by connetching the cathode and anode to the DC power supply. This forms an electrical circuit named as electrochemical cell circuit (ECC). The work piece is positioned beneath the tool electrode. As the applied voltage is provided to the ECC, hydrolysis takes place in the ECC. This evolves the H_2 bubble from the cathode and O_2 bubbles from the anode. The workpiece can be made as an anode if it is conductive in nature. This aids in the removal of material by anodic dissolution under heated electrolytes in the localized zone.[9]The tool electrode surface area is much smaller (approximately 100 times) compared to the surface area of auxiliary electrode, due to which the H_2 bubbles easily concentrate around the tool electrode. This forms a gas film around the immersed portion of the tool electrode. Since the film is non-conductive in nature, therefore it stops the flow of current in ECC. As a result, a high electrical field generates at the minimum cross-sectional area of the tool face (i.e., edge of the tool face). The breakdown of the H_2 gas film generates discharges and produces thermal energy. The generated thermal energy removes unwanted material by melting and vaporization.[10] However, the high thermal energy also evaporates water from the electrolyte while machining and leaves the sludge in the gap between the tool electrode and work material. Also, the chemical reactions that occurred in the gap due to the presence of electrolytes generate a passivation layer on the machined surface. It hampers the flow of current in the ECC. Therefore, the removal of sludge along with the passivation layer is essential to continue the machining process.[11] In order to tackle this problem, researchers have utilized an abrasive coated tool and revealed that the abrasive coated tool not only improves the material removal rate but also enhances the surface quality of machined features.[11, 12]Ladeesh and Manu reported that the use of grinding action in ECDM reduced the edge chipping at the exit side of the hole.[13] The assistance of grinding action with the ECDM process has been utilized to drill high aspect ratio micro holes of MMC[14] and glass[15]. Wang et al. investigated the surface integrity of alumina using the ECDM process with abrasive-coated wire.[16] They revealed that the use of abrasive-coated wire effectively removed the recast layer.

The information provided in the literature revealed that the abrasive coated tool could improve the process performance of the ECDM process, particularly for machining difficult-to-machine materials. In this regard, Jha et al. developed a new variant of the ECDM process in which an abrasive coated rotary disc electrode (ACRDE) was used for cutting and slitting MMC.[17]This investigation was performed to check the effectiveness of the ACRDE in the ECDM process. The effectiveness was measured in terms of cutting depth and width of cut. However, no information was found regarding the accuracy of cuts in the form of taper and overcut, which is essential to make any machining process industrially applicable. Apart from accuracy, productivity also needs to be analyzed simultaneously so that multiple objectives can be fulfilled at a time to expand the application area of MMCs. Therefore, by considering both the aspects of accuracy and productivity, the present research aims to analyze the grinding assisted-rotary disc-electrochemical discharge machining (GA-RD-ECDM) process during cutting Al-6063 SiC MMCs. The performance of the GA-RD-ECDM process was analyzed in terms of taper, width overcut (WOC), and material removal rate (MRR) by response surface methodology (RSM). Besides, analysis of variance (ANOVA) was performed to statistically analyze the developed regression models by RSM. Eventually, the GA-RD-ECDM process was optimized using the VIKOR (which stands for Vlse Kriterijumska Optimizacijal Kompromisno Resenje) methodology of multi-criteria decision-making by considering accuracy and productivity simultaneously. The confirmation experiments were also performed to validate the optimized process parameters.

The current findings can justify the GA-RD-ECDM facility as a low-cost solution of cutting of brittle and hard material as compare to laser, AJM, AWJM processes. The facility can also be used for high accuracy and productivity cutting operation, particularly for MMCs and other poor machinability/ difficult to machine materials such as glass, ceramic, etc. Thus, the outcomes of the present work may increase the industrial applicability of the GA-RD-ECDM process. This research work is organized into eight sections as follows:

Section one presents the application of MMCs followed by state-of-the-art literature review of ECDM and importance, significance and objectives of current research work. Section two focuses on the materials and method/ research methodology adopted for current investigation. This includes development of experimental facility of GA-RD-ECDM process, selection of input and output parameters, selection of workpiece material, tools and equipments used for measurement of responses and the experimental technique adopted for experimentation. Section three describes the preliminary experimentation in which different possible scenario of energy channelization behavior during GA-RD-ECDM of MMC are discussed. Section four emphasises on the discussion of experimental results, development of regression models for responses and analysis of variance. Section five deals with hybrid multi-response optimization of GA-RD-ECDM process. The responses are optimized using VIKOR methodology. Section six focuses on the conformation experiments. Section seven emphasises on the managerial implications of the current research work. Finally, Section eight presents the conclusions, limitation and future scope of the current study.

2 Materials and Methods

An in-house developed facility of the GA-RD-ECDM process was used in this research work. Figure 1 shows the schematic representation of the GA-RD-ECDM facility. The devolved facility comprisesfour components: DC pulsed power supply, tool electrode in the form of abrasive coated metallic disc, work holding device (i.e., fixture), and electrolyte chamber. In this facility, an abrasive coated rotary disc electrode (ACRDE) was utilized as a tool, and it was submerged into the electrolyte bath up to 2 mm. DC stepper motor rotated the ACRDE. Al-6063 SiCp MMC was used as a work material, which was fabricated by the stir casting process. The

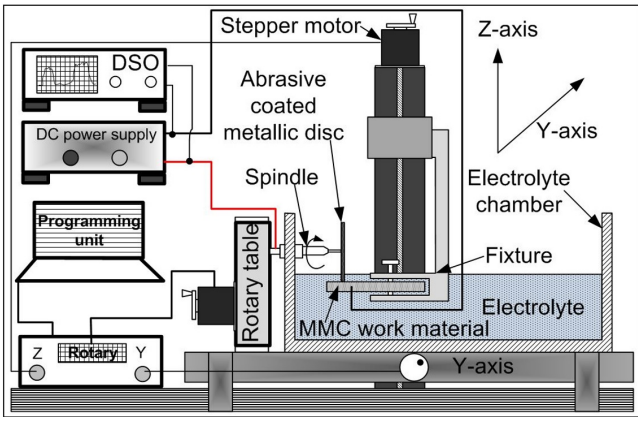

Fig. 1 — Schematic representation of GA-RD-ECDM Process.

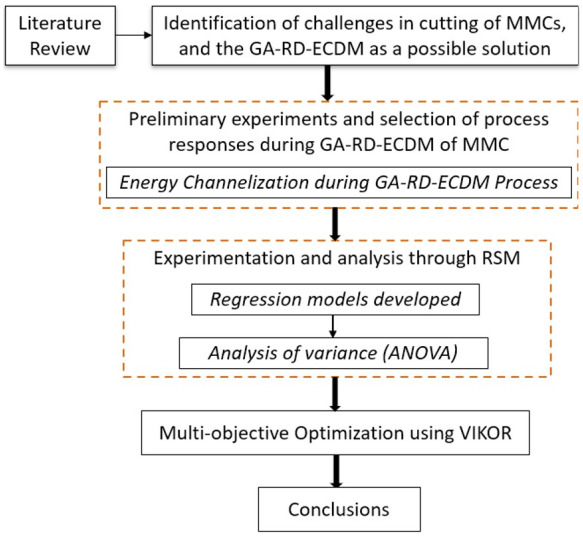

Fig. 2 — Research methodology.

casted Al-6063 SiCp MMC composition consists of Al, Si, C, and Mg in proportions of 87.72%, 4.20%, 4.80%, and 3.27%, respectively. A non-conductive fixture was used to hold the work material and placed beneath the rotating disc at a minimal working gap (i.e., almost zero).The research methodology adopted for this investigation is presented in the form of flow diagram shown in Fig. 2.

The work material was used as an anode (i.e., counter electrode). The $NaNO_3$ was selected as an electrolyte medium. The work material was fed by a numerically controlled Z-axis during machining, as shown in Fig. 1. The machining progress was recorded with the help of a digital storage oscilloscope (Make: Agilent, Model: DSOX3034A). The DSO was connected to the anode and cathode (Fig. 1). The experiments were designed and conducted by adopting response surface methodology. Four

input process variables: applied voltage, pulse on time, electrolyte concentration, and disc rotation speed were investigated during the GA-RD-ECDM process. The taper, WOC, and MRR were selected as responses, and their values were calculated using Eqs. (1)-(3) respectively.[17-19]

$$Taper\ (degree) = \frac{(W_1 - W_2)}{2d} \quad \ldots(1)$$

where, W_1 and W_2 are the width of slit at top surface and bottom surface respectively and d is the cutting depth of slit.

$$MRR\ (mg/min) = \frac{(w_i - w_f)}{t} \quad \ldots(2)$$

where, w_i and w_f are the weights of work material before and after machining and t is the machining time.

$$WOC\ (\mu m) = (W - T) \quad \ldots(3)$$

where, W and T are the width of slit and thickness of abrasive coated disk respectively.

2.1 Preliminary experiments: Energy channelization during GA-RD-ECDM process

In order to effectively utilize the GA-RD-ECDM process, a clear understanding of energy channelization during machining is essential. Without the proper use of energy, fabrication of a quality machined feature is impossible. Therefore, with this objective, pilot experimentation was conducted to investigate the energy channelization phenomenon during GA-RD-ECDM of MMC. This phenomenon is explained with the help of schematic representation shown in Fig. 3(a and b). Figure 3(a) shows the front view of the cutting operation of MMC work material using an abrasive coated rotary disc electrode (ACRDE) to fabricate slits. Figure 3(b) represents the side view of cutting operation to explain the mechanism of material removal in a better way. In Fig. 3(b) the frontal gap indicates the gap between the

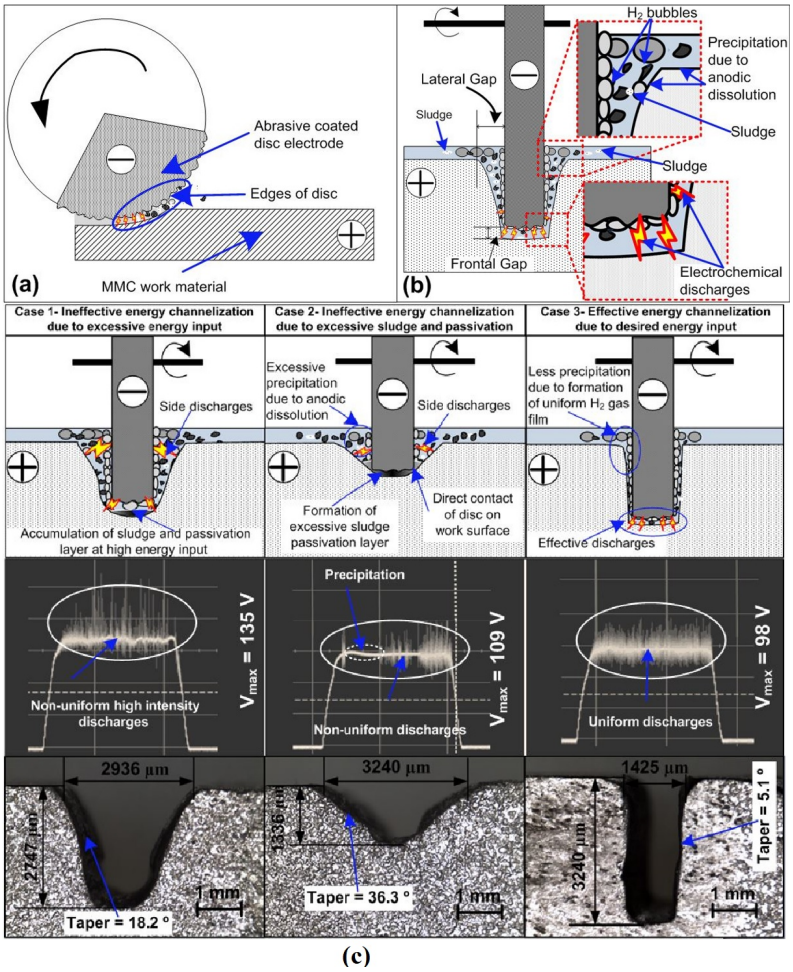

Fig. 3 — Schematic representation showing (a) front view (b) side view of cutting operation, and (c) different discharge behaviours of GA-RD-ECDM process along with captured DSO and microscopic images.

face of ACRDE and workpiece/work material. The lateral gap is shown in Fig. 3(b) indicates the gap between the sides of ACRDE and the vertical surface of the workpiece. The ACRDE is connected to a DC power supply as a cathode and MMC work material as an anode. Both the ACRDE and work material have physical contact with electrolytes. As the applied voltage was supplied to both the electrodes, an ECC formed in both the electrode and electrolyte. This generated H_2 bubbles from the cathode and O_2 bubbles from the anode. Anodic dissolution also took place in this process due to electrochemical dissolution, which formed the precipitates. Further, as the applied voltage increased the bubble generation intensified and as a result, H_2 gas film enveloped the ACRDE in the vicinity of the electrolyte.[20] The H_2 gas film stopped the flow of current in the ECC and intensified the electric field. Subsequently, the discharges initiated at the minimum possible gap between both the electrodes and resulted in thermal energy generation in the frontal gap shown in Fig. 3(b). The thermal energy removed the material from MMC by melting and vaporization. It also increased the electrolyte temperature between the gap of ACRDE and work material and contributed to accelerating the anodic dissolution of work material. However, the formation of the passivation layer also took place due to chemical action in the ECC. This deteriorated the process by ceasing the flow of current into the ECC. Although, the ACRDE provided additional assistance to the GA-RD-ECDM process for removal of the passivation layer and partial material removal by grinding action. Further, the preliminary experiments were also conducted to study the energy channelization behavior during GA-RD-ECDM of MMC. Three cases discussed the results of experimentation.

2.1.1 Case-1 Ineffective energy channelization due to excessive energy input

It was found that the combination of parameters resulting into excessive thermal energy during machining provided higher MRR but simultaneously deteriorated the quality of cut in the form of higher taper and WOC. The voltage signal and the microscopic image of the machined slit obtained at this parametric combination are presented in Fig. 3 (c) (i.e., case 1). It was because, at higher applied voltage, the rate of H_2 bubbles generation accelerated, forming a thick gas film in the vicinity of disc and electrolyte. The bursting of the thick gas film resulted in non-uniform high-intensity discharges, as shown in Fig. 3 (c) (i.e.,case 1). As a result, excessive thermal energy is generated in the machining zone.

2.1.2 Case-2 Ineffective energy channelization due to excessive sludge and passivation layer

It was found that the combination of parameters resulted in excessive sludge and passivation layer during machining, which hampered the discharge phenomena in the frontal gap leading to reduction MRR. Although, anodic dissolution in the lateral gap continued during machining, which produced excessive precipitation and resulted in higher taper and WOC. Higher electrolyte concentration is one of the primary reasons for the generation of excessive sludge and passivation layer. Additionally, a higher pulse on time also contributes to sludge and passivation layer formation by reducing the flushing/cooling time. It led to the generation of non-uniform discharges and excessive precipitation, as evidenced in Fig. 3 (c). As a result, a low thermal energy is produced. Apart from this, high disc rotation speed was also responsible for disturbing the discharge characteristics. This may lead to the direct contact of disc and work material, which may further dislodge the abrasives from the abrasive coated disc electrode.[17]

2.1.3 Case-3 Effective energy channelization due to desired energy input

It was found that the combination of parameters resulted in smooth and continuous machining (i.e., high MRR and low taper and WOC). The reason there of was the formation of uniform thin gas film at moderated applied voltage, pulse on time, disc rotation speed, and electrolyte concentration. The moderated rotation speed of the disc played a significant role in continuous sludge and passivation layer removal without affecting the discharging phenomena. This resulted in increased MRR. The formation of uniform discharges in the frontal gap reduced precipitation formation in the lateral gap, thereby reducing the taper and WOC. The continuous uniform discharges are evidenced in Fig. 3 (c).

3 Results and Discussion

3.1 Analysis of taper, MRR, and WOC during GA-RD-ECDM process

Machining accuracy and productivity both are vital attributes of a machining process. The accuracy is analyzed in terms of taper and WOC, whereas productivity is analyzed in terms of MRR. For precision machining, both the taper and WOC should be as minimal as possible. At the same time, higher productivity in terms of higher MRR is always desired.

Thus, in this investigation, Taper, WOC, and MRR were analyzed to use the GA-RD-ECDM process as a precision machining process. The experimentation was performed as per the experimental settings given in Table 1. The results are furnished in Table 2.

The analysis of variance (ANOVA) was performed using Design expert software, and the regression models were developed. The summary of ANOVA results for taper, MRR, and WOC are tabulated in Table 3. The results of ANOVA revealed that the value of deterministic coefficients for taper, MRR, and WOC were higher than 95% and the Prob. > F value of models for taper, MRR and WOC were significant at 95% confidence level. All the input process variables of GA-RD-ECDM process selected in this investigation were statistically significant. The lack of fit term was insignificant term for all the response measures. In Table 3, low Prob. > F value of the model and high Prob. > F value of lack of fit for all the response measures indicates the developed models' statistical significance. The insignificant terms are having Prob. > F value greater than 0.05 was eliminated using the backward elimination method. The regression models developed for taper, MRR and WOC are presented in Eq. (4)-(6), respectively.

Table 1 — Process parameter settings

Variable parameters	Symbol	Units	Levels		
			-1	0	1
Applied voltage	A	V	55	60	65
Pulse-on time	B	ms	3	3.25	3.5
Electrolyte concentration	C	% wt/vol.	25	30	35
Disc rotation speed	D	rpm			
Constant parameters					
Electrolyte		N_aNO_3			
Machining duration		10 min.			
Pulse-off time		1 m-second			
Thickness of rotating disc		700 µm			

Table 2 — Experimental design with performance measures

Exp. No.	Process parameters				Performance measures		
	A	B	C	D	Y_1	Y_2	Y_3
1	85	2.5	18	30	5.92	3.74	652
2	115	2.5	18	30	8.46	3.97	682
3	85	3.5	18	30	7.04	3.94	680
4	115	3.5	18	30	9.58	4.17	710
5	100	3	12	15	8.00	3.70	660
6	100	3	24	15	11.37	3.85	683
7	100	3	12	45	9.00	4.20	685
8	100	3	24	45	12.37	4.35	707
9	85	3	18	15	9.31	3.69	675
10	115	3	18	15	11.85	3.92	705
11	85	3	18	45	10.31	4.20	700
12	115	3	18	45	12.85	4.42	730
13	100	2.5	12	30	4.61	3.68	637
14	100	3.5	12	30	5.74	3.95	665
15	100	2.5	24	30	7.99	3.90	660
16	100	3.5	24	30	9.11	4.10	687
17	85	3	12	30	6.64	3.75	678
18	115	3	12	30	9.18	3.97	707
19	85	3	24	30	10.02	3.90	700
20	115	3	24	30	12.56	4.25	730
21	100	2.5	18	15	7.25	3.69	635
22	100	3.5	18	15	8.40	3.89	662
23	100	2.5	18	45	8.27	4.20	660
24	100	3.5	18	45	9.40	4.40	687
25	100	3	18	30	4.28	4.29	637
26	100	3	18	30	4.26	4.30	639
27	100	3	18	30	4.27	4.31	638
28	100	3	18	30	4.29	4.28	636
29	100	3	18	30	4.27	4.26	635

A: Applied voltage (V), B: Pulse-on time (µ-second), C: Electrolyte concentration (%wt/vol.), D: Disc rotation speed (rpm), Y_1: Taper (degree), Y_2: MRR (mg/min), Y_3: WOC (µm)

Table 3 — ANOVA Results for MRR, taper and WOC

ANOVA Results for MRR

Source	Sum of squares	Degree of freedom	Mean square	F value	Prob. > F	
Model	1.62	14	0.12	178.73	< 0.0001	Significant
Residual	0.00903	14	0.00064	-	-	-
Lack of fit	0.00755	10	0.00075	2.04	0.2562	Not significant
Pure error	0.00148	4	0.00037	-	-	
Cor. total	1.62	28	-	-	-	-

Standard deviation = 0.025, Mean = 4.04, Coefficient of variation = 0.63, Predicted residual error of sum of squares = 0.046, R^2 = 0.9944, Adjoint R^2 = 0.9889, Predicted R^2 = 0.9718, Adequate precision = 42.023.

ANOVA Results for taper

Source	Sum of squares	Degree of freedom	Mean square	F value	Prob. > F	
Model	204.77	14	14.63	4032.85	< 0.0001	Significant
Residual	0.051	14	0.00362	-	-	-
Lack of fit	0.047	10	0.00467	4.68	0.0752	Not significant
Pure error	0.004	4	0.001	-	-	
Cor. total	204.82	28	-	-	-	-

Standard deviation = 0.06, Mean = 8.16, Coefficient of variation = 0.74, Predicted residual error of sum of squares = 0.28, R^2 = 0.9998, Adjoint R^2 = 0.9995, Predicted R^2 = 0.9987, Adequate precision = 198.348.

ANOVA Results for WOC

Source	Sum of squares	Degree of freedom	Mean square	F value	Prob. > F	
Model	204.77	14	14.63	4032.85	< 0.0001	Significant
Residual	0.051	14	0.00362	-	-	-
Lack of fit	0.047	10	0.00467	4.68	0.0752	Not significant
Pure error	0.004	4	0.001	-	-	
Cor. total	204.82	28	-	-	-	-

Standard deviation = 1.34, Mean = 674.83, Coefficient of variation = 0.20, Predicted residual error of sum of squares = 103.47, R^2 = 0.9989, Adjoint R^2 = 0.9979, Predicted R^2 = 0.9957, Adequate precision = 98.703.

$$\text{Taper} = 174 - 2.70411 \times A - 8.00667 \times B - 1.96653 \times C - 0.98178 \times D + 0.0133 \times B \times D + 0.01395 \times A^2 + 1.4700 \times B^2 + 0.06201 \times C^2 + 0.01650 \times D^2 \pm \varepsilon \quad \ldots(4)$$

$$\text{MRR} = -12.7461 + 0.13265 \times A + 4.71267 \times B + 0.18358 \times C + 0.03745 \times D + 0.000361 \times A \times C - 0.00065 \times A^2 - 0.7326 \times -0.00519 \times C^2 - 0.00032 \times D^2 \pm \varepsilon \quad \ldots(5)$$

$$\text{WOC} = 2627.3240 - 36.9259 \times A - 1.3333 \times B - 20.6250 \times C - 5.1000 \times D - 0.5000 \times B \times C + 0.1901 \times A^2 + 6.1666 \times B^2 + 0.6851 \times C^2 + 0.0996 \times D^2 \pm \varepsilon \quad \ldots(6)$$

where, A, B, C, D and ε are the applied voltage in volt, pulse on time in ms, electrolyte concentration in % wt./vol., disc rotation speed in rpm and error, respectively.

3.2 Effect of applied voltage on responses

Applied voltage plays a significant role in the ECDM process while machining of any material. It governs the energy input in the machining zone. The effect of applied voltage on responses (i.e., MRR, WOC and taper) are plotted in Fig. 4 (a-c), respectively. Figure 4 (a) indicates that an increase in the applied voltage from 85 V to 115 V increased the MRR. It was because increasing the applied voltage in the ECC increased the generation of discharges from the edges of the abrasive coated disc. This accelerated thermal energy generation in the machining zone and thereby morematerial removal from work material. On the other hand, the WOC and taper decreased as the applied voltage increased up to 100 V, and after that, an increasing trend was noticed in WOC and taper (Fig. 4 (b and c)). The reason for this trend was that as the applied voltage increased up to 100 V, the

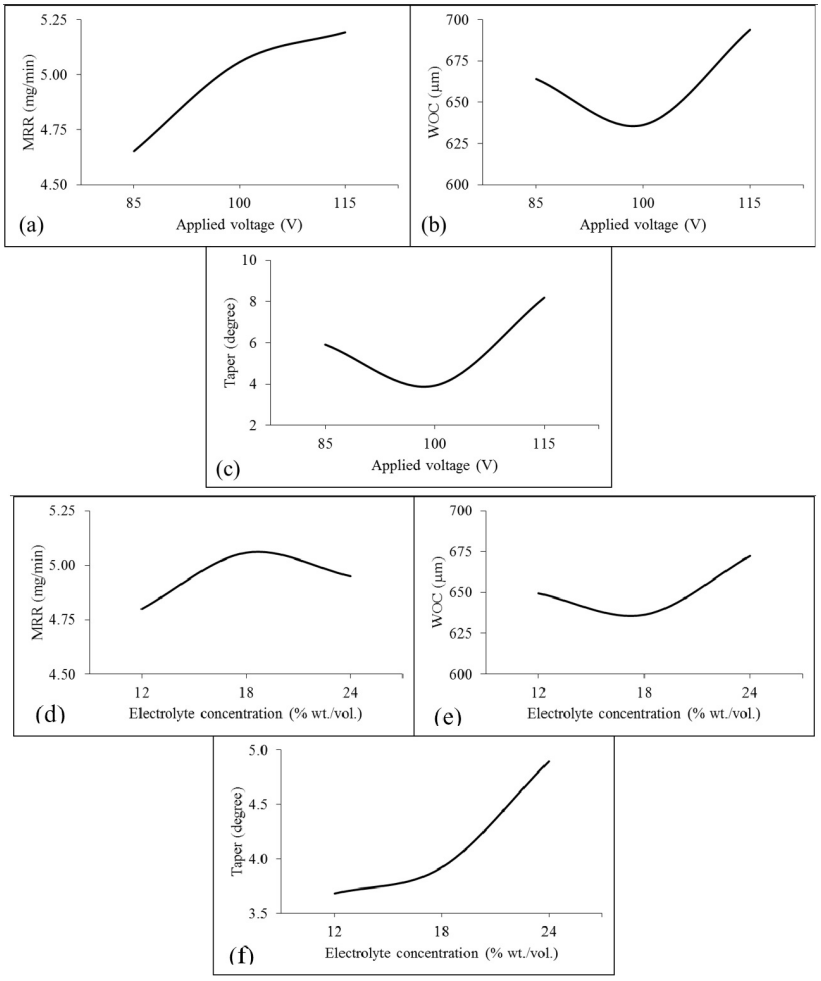

Fig. 4 — Effect of applied voltage and electrolyte concentration MRR, WOC, and taper .

generated thermal energy by discharge effectively channelized on the work material leading to the lowest WOC and taper (Case-3 shown in Fig. 3 (c)). But, beyond 100 V of applied voltage, the rate of H_2 bubble formation increased disc surface immersed into the electrolyte. This resulted in the formation of discharges in the frontal as well as the lateral gap leading to the generation of excessive thermal energy (Case-1 shown in Fig. 3 (c)) and hence higher WOC and taper.

3.3 Effect of electrolyte concentration on responses

The electrolyte is essential to establish ECC during the ECDM process. The concentration of electrolyte provides strength to ECC. Increasing the electrolyte concentration increased the intermolecular conductivity between the electrodes and vice-versa.[16] Although, it has another adverse effect on responses. The effect of electrolyte concentration on MRR, WOC and taper of slit is presented in Fig. 4(d-f), respectively. Figure 4(d and e)indicate that as the electrolyte concentration increased from 12% to 18%, MRR increased whereas the WOC was observed to decrease. Also, the taper slightly increased. The reason thereof was that increasing the electrolyte concentration increased the intermolecular conductivity between the electrodes. It increased the intensity of discharges and increased thermal energy in the frontal gap during the ECDM process (case 4 shown in Fig. 3 (c)). However, on further increasing the electrolyte concentration from 18% to 24 %, MRR was found to be decreased (Fig. 4(d)), whereas both the WOC and taper increased (Fig. 4 (e and f)). It was due to the formation of excessive sludge and passivation layer (case-1 shown in Fig. 3 (c)).

3.4 Effect of pulse on time on responses

Pulsed DC power supply has been adopted over continuous DC power supply. It provides discontinuity on the ECDM process called pulse off

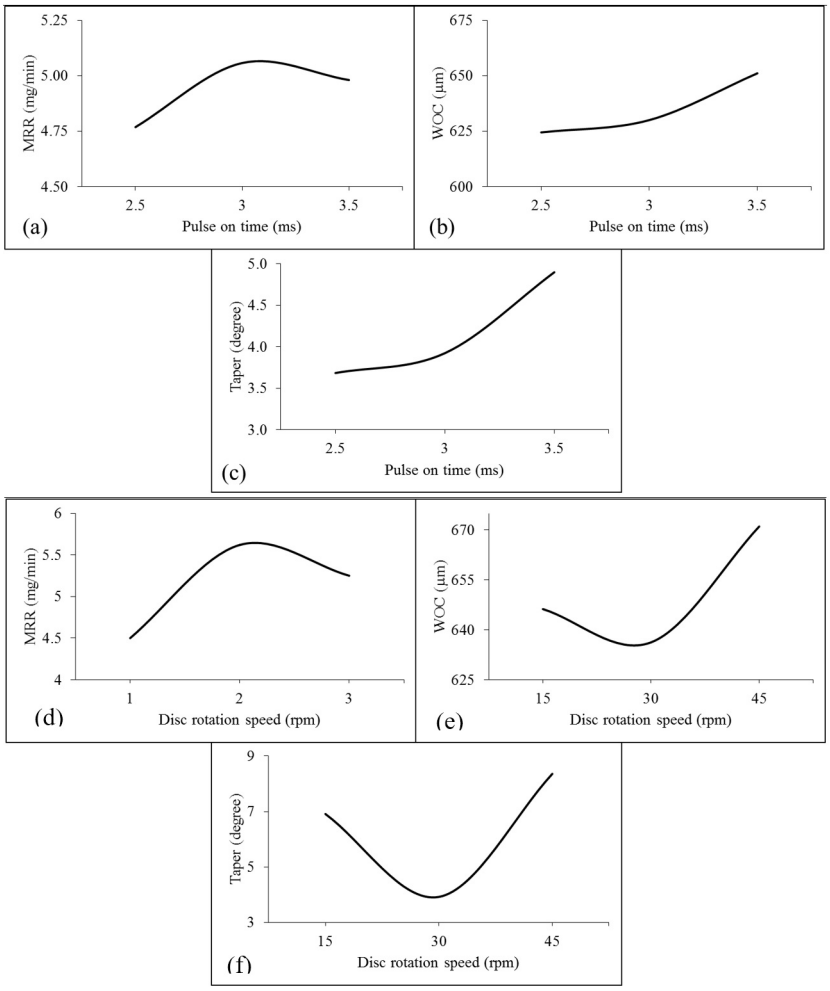

Fig. 5 — Effect of pulse on time and disc rotation speed on MRR, WOC, and taper .

time for cooling of work material and flushing of sludge and debris from machining area. The active duration of the ECDM process is called pulse-on-time. A proper combination of pulse-on-time and pulse-off-time is required to attain desired output. Hence, the investigation is performed to discuss the effect of pulse on time on MRR, WOC, and taper of a slit at a fixed value of pulse off time are illustrated in Fig. 5 (a-c) respectively. Figures 5 (a and b) showed that on increasing the pulse on time from 2.5 ms to 3.0 ms, the MRR, WOC, and taper increased. The increasing trend was due to the generation of thermal energy. Nevertheless, beyond 3.0 ms, pulse-on-time showedan adverse effect on all the responses, i.e., MRR, WOC and taper. The reason was that at a higher level of pulse on time, discharging occurred for a longer duration and generated higher thermal energy in the frontal gap. This led to the formation of excessive sludge and passivation layer (case-1, Fig. 3 (c)) in the machining area. Moreover, a higher pulse on time led to discharging and precipitation in the lateral gap.

3.5 Effect of disc rotation speed on responses

In the GA-RD-ECDM process, the rotation of disc provides additional assistance of grinding action to the ECDM process, which helps remove the sludge and passivation layer in the machining area. However, at a very high disc rotation speed, it harms responses by deteriorating the stability of H_2 gas film. Eventually, the non-uniform discharges generate. It can be seen from Fig. 5 (d-f) that increasing the disc rotation speed from 15 rpm to 30 rpm increased MRR and decreased the WOC and taper. After 30 rpm, the MMR increased, whereas both the WOC and taper increased.

In order to make an experimental investigation complete, the combined effect of input process parameters on process performance is necessary. With

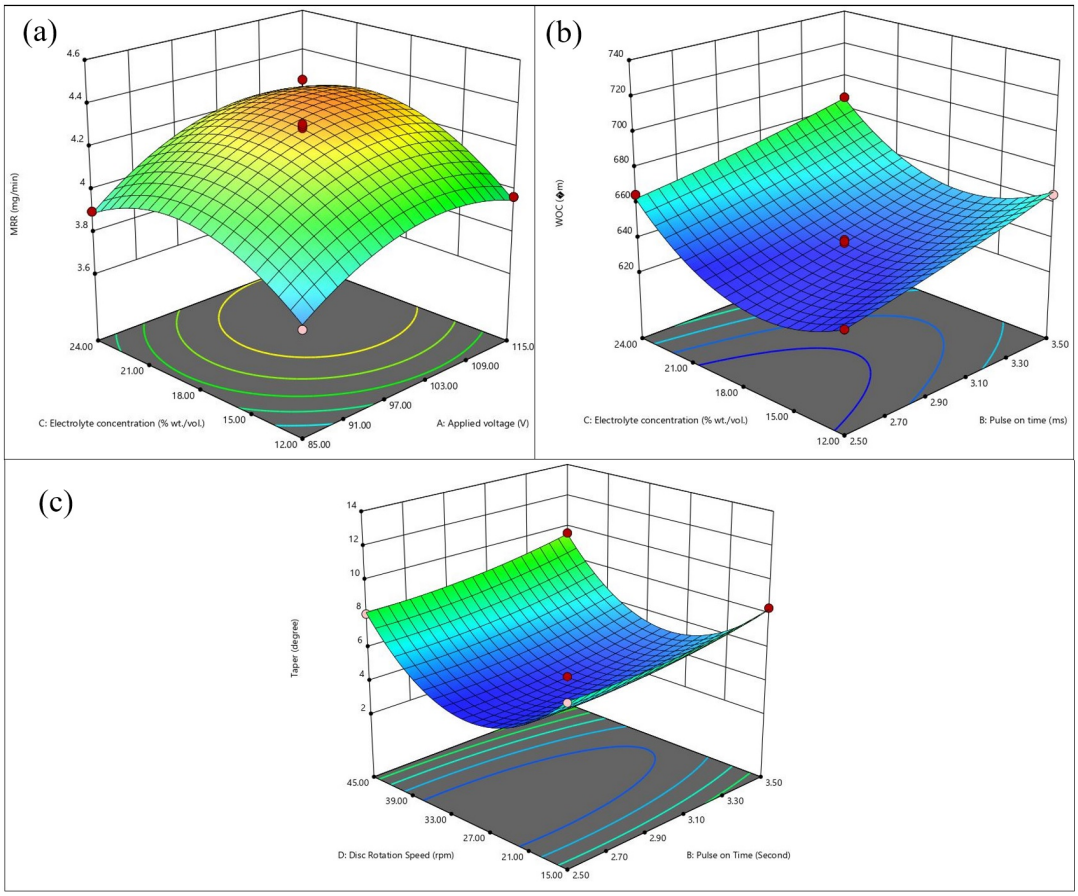

Fig. 6 — Combined effect of (a) electrolyte concentration and applied voltage on MRR, (b) electrolyte concentration and pulse on time on WOC, and (c) disc rotation speed and pulse on time on taper

this objective, the combined effect of input parameters is also observed during the machining of MMC using the GA-RDECDM process. The interaction effect of applied voltage and electrolyte concentration on MRR is shown in Fig. 6 (a). A simultaneous increase in applied voltage and electrolyte concentration increased the MRR up to a particular value. After that, a decreasing trend can be observed. This was because increasing both the process parameters increased the amount of thermal energy in the machining zone as well as the sludge and passivation layer. Hence, the increased amount of thermal energy increased the MRR. However, with the higher value of applied voltage and electrolyte concentration, the discharge phenomena hampered due to excessive sludge and passivation layer formation, which lowered the MRR.

The mutual effect of pulse-on-time and concentration of electrolyte on WOC is shown in Fig.6 (b). As can be seen that the WOC gradually increased by increasing the pulse on time at all values of electrolyte concentration. It was because the duration of thermal energy generation increased by increasing pulse on time at all values of electrolyte concentration. Nevertheless, increasing the electrolyte concentration up to mid-level decreased the WOC and, after that, increased the WOC. The reason for the same was that an increase in electrolyte concentration improved the discharging behavior by increasing intermolecular conductivity. However, it also increased the sludge and passivation layer formation, which deteriorated the discharging behavior after a certain value of electrolyte concentration and increased the WOC. Minimum WOC was obtained at mid-level of electrolyte concentration along with a low level of pulse on time.

The mutual effect of disc rotation speed and pulse-on-time on the taper of the slit is shown in Fig. 6 (c). It can be observed that the combination of low disc rotation speed led to high taper. Similarly, very high disc rotation speed and pulse on time also led to the high taper. It was due to the ineffective removal of sludge. The minimum taper was observed at the mid-

level of both the input parameters. It was because effective removal of the passivation layer, sludge, and debris was accomplished by increasing the disc's rotation speed. However, increasing the disc rotation speed to the higher values resulted in a high taper with all the pulse values on time because at a very high disc rotation speed, H_2 gas film deteriorated. This may result in direct contact of a disc on the work surface and discharges in the lateral gap. Also, the increasing pulse-on-time increased the taper slightly for all the values of disc rotation speed.

3.6 Multi-objective Optimization using VIKOR

The multi-criteria decision-making (MCDM) is an effective way to solve the problems of multi-response optimization. It is extensively used when the best solution is desired among several alternatives having more than one attribute (i.e., process outcomes).[21] In all the MCDM methodologies, the problem is expressed in terms of a decision matrix, as shown by Eq. (7). This decision matrix contains 'a' number of alternatives (i.e., experimental settings) and 'b' number of criteria (i.e., responses). In this investigation 29 alternatives and 3 criteria were selected.

$$D = \begin{bmatrix} x_{11} & x_{12} \cdots & \cdots & x_{1b} \\ x_{21} & x_{22} \cdots & \cdots & x_{2b} \\ \vdots & \vdots \ddots & & \ddots \vdots \\ \vdots & \vdots \ddots & & \ddots \vdots \\ \vdots & \vdots \ddots & & \ddots \vdots \\ x_{a1} & x_{a2} \cdots & \cdots & x_{ab} \end{bmatrix} \quad \ldots(7)$$

where, x_{ij} indicates the value of j^{th} attribute of i^{th} trial.

VIKOR comes under the category of MCDM tools. The complete procedure of obtaining the optimal solution of an MCDM problem using VIKOR methodology is comprised of four steps and discussed subsequently.

Step-1: Normalization of decision matrix.

The purpose of normalization is to make the responses free from their units. Equation (8) represents the normalized decision matrix that was determined by using Eq. (9).

$$K = \left[k_{ij}\right]_{a\times b} \quad \ldots(8)$$

$$k_{ij} = \frac{x_{ij}}{\sqrt{\sum_{j=1}^{b} {x_{ij}}^2}}\ j = 1, 2 \ldots., b \quad \ldots(9)$$

where, k_{ij} indicates the normalized value of j^{th} attribute for i^{th} trial and x_{ij} represents the value of i^{th}response corresponding to j^{th} attribute.

3.6.2 Step-2 Determination of ideal best and ideal worst solutions

The ideal best solution and ideal worst solutions are the most desired and most undesired values of the responses respectively. For instant, in case of taper, the minimum value of taper obtained from all the experiments is the ideal best solution, whereas the maximum value of taper is the ideal worst solution. Both of these solutions were demined using Eq. (10) and Eq. (11).

$$K^* = \left[\left(\max \quad K_{ij} \middle| j \in \mathrm{J}\right), \left(\left(\min \quad K_{ij} \middle| j \in \mathrm{J}'\right) \middle| i = 1, 2, \ldots, a\right)\right] = \{k_1^*, k_2^*, k_3^*, \ldots\ldots, k_b^*\} \quad \ldots(10)$$

$$K^- = \left[\left(\min \quad K_{ij} \middle| j \in \mathrm{J}\right), \left(\left(\max \quad K_{ij} \middle| j \in \mathrm{J}'\right) \middle| i = 1, 2, \ldots, a\right)\right] = \{k_1^-, k_2^-, k_3^-, \ldots\ldots, k_b^-\} \quad \ldots(11)$$

where, $J = (j = 1, 2, \ldots., a | K_{ij}$, larger value of response is desired) and $J' = (j = 1, 2, \ldots., a | K_{ij}$, a smaller value of response is desired).

The ideal best and worst solutions obtained in this investigation were 0.0922 and 0.2783 for taper, 0.2026 and 0.1687 for MRR, and 0.1747 and 0.2008 for WOC.

3.6.3 Step-3 Calculation of utility and regret measures

The utility and regret measures corresponding to each alternative were computed using Eq. (12) and Eq. (13), respectively.

$$S_i = \sum_{j=1}^{a} w_j\left(k_j^* - k_{ij}\right)/\left(k_j^* - k_j^-\right) \quad \ldots(12)$$

$$R_i = Max\left[w_j\left(k_j^* - k_{ij}\right)/\left(k_j^* - k_j^-\right)\right] \quad \ldots(13)$$

where, S_i indicates the utility measure, R_i indicates the regret measure, and w_j indicates the weight assigned to the j^{th} criterion. In this investigation, the weights assigned to the taper, MRR, and WOC were 0.5, 0.2, and 0.3, respectively. The prime importance was to the accuracy (i.e., taper) over productivity (i.e., MRR). Thus maximum weight was assigned to the taper followed by WOC and MRR.

3.6.4 Step-4: Calculation of VIKOR index

This is the final step of the VIKOR method. VIKOR index (V_i) corresponding to all experimental settings were calculated using the value of utility measures and regret measures computed in the previous step. Equation (14) was used to calculate the VIKOR index with respect to each experimental run.

$$V_i = u\left[\frac{S_i - S^*}{S_i^- + S^*}\right] + (1-u)\left[\frac{R_i - R^*}{R_i^- + R^*}\right] \quad \ldots(12)$$

where, V_i indicates the VIKOR index corresponding to $i^{th}$the alternative. The value of VIKOR index lies between 0 and 1 (i.e. $0 \leq V_i \leq 1;\ i = 1, 2, \ldots \ldots, a$). S^* is the minimum value of S_i and S^- is the maximum value of S_i. Similarly, R^* is the minimum value of R_i and R^- is the maximum value of R_i. The parameter u represents the weight of the maximum group utility. In this investigation, the values ofS^*, R^*, $S^-$and R^- were obtained were 0.0398, 0.0297, 0.8291 and 0.5000 respectively. A value of 0.5 was selected for u.[22-24] The VIKOR index are presented in Table 4.

After computing the VIKOR index, the experiential settings are ranked in the increasing order of VIKOR index. The alternative (i.e., experimental setting) with respect to the smallest VIKOR index is determined as the optimal solution. On the basis of the VIKOR index tabulated in Table 4, the experiment number 27 resulted in smallest VIKOR index (i.e., 0.000), thus it was assigned 1st rank. Therefore, the optimal parametric settings obtained as applied voltage = 100 V, pulse on time = 3 µ-second, concentration = 18% wt/vol. and disk rotation speed = 30 rpm for minimum taper and WOC and maximum MRR.

Table 4 — Unity measure, regret measure VIKOR index and rank

Unity measure (Si)	Regret measure (Ri)	VIKOR index (Qi)	Rank
0.463	0.403	0.350	8
0.472	0.256	0.529	16
0.538	0.338	0.390	10
0.547	0.199	0.661	22
0.343	0.282	0.486	14
0.256	0.101	0.839	25
0.540	0.224	0.549	17
0.451	0.272	0.900	26
0.294	0.206	0.647	20
0.303	0.147	0.918	27
0.495	0.211	0.708	23
0.500	0.300	0.982	28
0.484	0.480	0.299	7
0.586	0.414	0.273	6
0.425	0.283	0.451	13
0.497	0.218	0.581	19
0.480	0.361	0.424	11
0.483	0.214	0.650	21
0.391	0.165	0.731	24
0.448	0.231	0.982	29
0.330	0.326	0.388	9
0.401	0.259	0.497	15
0.530	0.267	0.427	12
0.602	0.292	0.558	18
0.750	0.499	0.008	3
0.760	0.500	0.006	2
0.761	0.499	0.000	1
0.744	0.498	0.010	4
0.735	0.499	0.017	5

3.7 Conformation Experiments

The validation of optimal parametric combination through conformation experiments is essential to examine the repeatability of the process outcomes. Therefore, three conformation trials were performed at optimal parametric combination (i.e., applied voltage = 100V, pulse on time = 3 µ-second, concentration = 18% wt/vol. and disk rotation speed = 30 rpm). The responses were measured in terms of taper, MRR and WOC and tabulated in Table 5. The closeness between both the results ensures the repeatability and effectiveness of optimal parametric results.

Further, to determine the order of significance of input parameters affecting the process performance, the difference between maximum and minimum VIKOR index was calculated and tabulated in Table 5. The difference between maximum and minimum VIKOR index for applied voltage, pulse on time, electrolyte concentration, and disc rotation speed were obtained as 0.417, 0.114, 0.330, and 0.313, respectively. The highest value of difference indicates the most significant parameter, whereas the lowest value indicates the least significant parameter affecting the process responses. Thus, it can be clearly seen that applied voltage with the highest delta value most significantly affected the performance of the GA-RD-ECDM process. The order of significant parameters was as applied voltage followed by electrolyte concentration, disk rotation speed, and pulse on time.

3.8 Managerial Implications

The current work provided an effective solution as the GA-RD-ECDM process for the cutting of Al-6063 SiCp MMC. To increase the industrial applicability of the process, parametric evaluation using RSM and optimization using the VIKOR method was also performed. Although the current investigation is limited to slit cutting of Al-6063 SiC MMC, in the future, the process can be used for other machining operations, and for other materials. Even though there are many machining processes available in the commercial domain, most are facing issues like high investment/running cost and low productivity. The GA-RD-ECDM has the potential to come up with an effective solution. Eventually, organizations or entrepreneurs can utilize the information provided in the present work for the commercialization of the GA-RD-ECDM process.

Table 5 — Results of confirmation experiments and Means of VIKOR Index

Responses	Confirmation experiments: Experimental conditions (Applied voltage = 100 V, pulse on time = 3 μ-second, electrolyte concentration = 24% wt./vol., , disc rotation speed = 30 rpm)			
	Exp. 1	Exp. 2	Exp. 3	Average
Taper (°)	4.26	4.30	4.32	4.28
MRR (mg/min)	4.31	4.26	4.28	4.27
WOC (μm)	638	625	642	635

Means of VIKOR Index

Parameters	Average VIKOR index			Max-Min	Rank
	Level 1	Level 2	Level 3		
Applied voltage	0.542	0.370	0.787	0.417	1
Pulse on time	0.407	0.521	0.493	0.114	4
Concentration	0.447	0.417	0.747	0.330	2
Disk rotation speed	0.629	0.374	0.687	0.313	3

4 Conclusion

This research was aimed at performance analysis of GA-RD-ECDM process during cutting of slits on Al-60630 MMC. The performance was analyzed through extensive experimentation designed by using RSM. Additionally, multi-objective optimization was performed to achieve multiple objectives such as lower taper and WOC and higher MRR at a time. The conclusions drawn on the basis of results and discussion are as follows:

- The integration of grinding action and disc rotation augmented the performance of ECDM process in terms of reduced taper and WOC and increased MRR by providing uniform removal of material.
- Both very low and high values of disc rotation speed and applied voltage deteriorates the accuracy of the slits by increasing taper and WOC.
- The lower value of pulse-on-time and electrolyte concentration provided better control on accuracy (i.e., lesser taper and WOC) of the slitsbut at a low machining rate.
- The combination of disc rotation speed and pulse on time, electrolyte concentration and pulse on time, and electrolyte concentration and applied voltage significantly affected the taper, WOC, and MRR.
- All the input process variables were statistically significant for taper, MRR, and WOC at a 95% confidence level. The applied voltage was the most significant variable affecting the performance of the GA-RD-ECDM process.
- The integration of RSM and VIKOR, the optimum parametric setting for lower taper and WOC, and higher MRR was determined as applied voltage = 100 V, pulse-on time = 3 μ-second, electrolyte concentration = 18% wt/vol. and disk rotation speed = 30 rpm.The GA-RD-ECDM process can be employed for cutting slits on other conductive and insulating materials for optical and heat transfer applications.
- The present work provided insight into the effective use of the GA-RD-ECDM process for the cutting of Al-60630 MMC. Similarly, in future, the GA-RD-ECDM process can be explored for other advanced materials (i.e., glass, polymer composites and ceramics) for fabrication of microchannels for microfluidic applications.

Acknowledgments

The authors are highly grateful to MIED, Indian Institute of Technology Roorkee, India for conducting this research work.

References

1 Dvivedi A, Rajeev V R, Kumar P, & Singh I, *Proc Inst MechEng Part J, J Eng Tribo,* 226 (2012) 138.
2 Satish Kumar D, Kanthababu M, Vajjiravelu V, Anburaj R, Sundarrajan N T, & Arul H, *Int J Adv Manuf Technol*, 56 (2011) 975.
3 Etemadi R, Wang B, Pillai K M, Niroumand B, Omrani E, & Rohatgi P, *Mater Manuf Process*, 33(12) (2017) 1261.
4 Sidhu S S, Kumar S, & Batish A, *Crit Rev Solid State Mater Sci*, 41 (2016) 132.
5 Nicholls C J, Boswell B, Davies I J, & Islam M N, *Int J Adv Manuf Technol*, 90 (2017) 2429.
6 Singh S, Singh I, & Dvivedi A, *Proc Inst Mech Eng Part B, J Eng Manuf*, 227 (2013) 1767.
7 Arya R K, & Dvivedi A, *J Mater Process Technol*, 266 (2019) 217.
8 Goud M, Sharma AK, & Jawalkar C, *Precis Eng,* 45 (2016) 1.
9 Huang S F, Liu Y, Li J, Hu H X, & Sun L Y, *Mater Manuf Process*, 29 (2014) 634.

10 Singh T, & Dvivedi A, *Int J Mach Tools Manuf*, 105 (2016) 1.
11 Liu J W, Yue T M, & Guo Z N, *Mater Manuf Process*, 24 (2009) 446.
12 Wei C, Hu D, Xu K, & Ni J, *Int J Mach Tool Manuf,* 51(2) (2011) 165.
13 Ladeesh V G, & Manu R, *Adv Manuf,* 6(2) (2018) 215.
14 Singh T, Arya R K, & Dvivedi A, *Mach Sci Technol,* 24 (2019) 195.
15 Arya RK, & Dvivedi A, *Thermal loading effect during machining of borosilicate glass using ECDM process*, paper presented at 4th International Conference on Advanced Materials Research and Manufacturing Technologies (AMRMT 2019), Oxford, UK, 2019.
16 Wang J, Fu C, & Jia, Z, *J Mater Process Technol,* 252 (2018) 225.
17 Jha N K, Singh T, Dvivedi A, & Rajesha S, *Mater Manuf Process, 34*(3) (2019) 243.
18 Kumar S, & Dvivedi A, *Mat Sci Semicon Proc* 102 (2019) 104584.
19 Kumar S, & Dvivedi A, *Mater Manuf Process,* 34(5) (2019) 475.
20 Behroozfar A, & Razfar M R, *Mater Manuf Process,* 31 (2016) 574.
21 Zeleny M, Multiple criteria decision making (McGraw-Hill, New York), ISBN: 0070727953, 1982, p. 152.
22 Jalilibal Z, Bozorgi-Amiri A & Khosravi R, *J Proj Manag* 33 (2018) 131.
23 Sanayei AS, Farid M, & Ahmad Y, *Expert Sys Appl* 37(1) (2010) 24.
24 Tong L I, Chen C C, & Wang C H, *Int J Adv Manuf Technol* 31(11-12) (2007) 1049.